PHYSICAL REVIEW A **85**, 011402(R) (2012)

Routes to formation of highly excited neutral atoms in the breakup of strongly driven H_2

A. Emmanouilidou,[1,2] C. Lazarou,[1] A. Staudte,[3] and U. Eichmann[4,5]

[1]*Department of Physics and Astronomy, University College London, Gower Street, London WC1E 6BT, United Kingdom*

[2]*Chemistry Department, University of Massachusetts at Amherst, Amherst, Massachusetts 01003, USA*

[3]*Joint Laboratory for Attosecond Science, University of Ottawa and National Research Council, 100 Sussex Drive, Ottawa, Ontario, Canada K1A 0R6*

[4]*Max-Born-Institute, Max-Born-Strasse 2a, D-12489 Berlin, Germany*

[5]*Institut für Optik und Atomare Physik, Technische Universität Berlin, D-10632 Berlin, Germany*

(Received 9 November 2011; published 11 January 2012)

We present a theoretical quasiclassical treatment of the formation, during Coulomb explosion, of highly excited neutral H atoms (H^*) for strongly driven H_2. This process, where after the laser field is turned off, one electron escapes to the continuum while the other occupies a Rydberg state, was recently reported in an experimental study [B. Manschwetus *et al.*, Phys. Rev. Lett. **102**, 113002 (2009)]. We find that two-electron effects are important in order to correctly account for all pathways leading to H^* formation. We identify two pathways where the electron that escapes to the continuum does so either very quickly or after remaining bound for a few periods of the laser field. These two pathways of H^* formation have distinct traces in the probability distribution of the escaping electron momentum components.

DOI: 10.1103/PhysRevA.85.011402 PACS number(s): 33.80.Rv, 34.80.Gs, 42.50.Hz

A wealth of physical phenomena is manifested during fragmentation of molecules driven by intense infrared laser fields. Already in the simplest diatomic molecule H_2 many of the archetypical molecular fragmentation mechanisms are present, such as bond softening and above-threshold dissociation [1,2], molecular nonsequential double ionization (NSDI) [3–6], and enhanced ionization (EI) [6,7]. Very recently, another interesting phenomenon, the formation of highly excited neutral fragments, has been observed in strongly driven H_2 [8] and other molecules [9]. This formation of excited fragments has been attributed to "frustrated tunnel ionization" [10].

Here, we report a theoretical study of the mechanisms leading to the formation of highly excited H atoms (H^*) during "frustrated" double ionization (since only one electron eventually escapes) of H_2 driven by intense, infrared laser fields. Specifically, we present a theoretical treatment of H^* formation accounting for the motion of the two electrons and the nuclei. In Ref. [8], it was conjectured that the interaction of the H_2^+ ion alone with the laser field, and thus solely one-electron effects, can account for the breakup of H_2 into a proton, a Rydberg atom, and an escaping electron. In this Rapid Communication we show that this is only partly true and that two-electron effects are important in order to correctly account for all pathways leading to H^* formation. We identify two distinctly different routes to forming H^* depending on which one of the two ionization steps is "frustrated." We find that these two pathways have distinct traces in the observable final momentum components of the escaping electron. Exploiting these different traces one can experimentally separate, to a certain extent, one pathway from the other.

Accounting for both electronic and nuclear motion is a challenging task. Previous theoretical studies of strongly driven H_2 either used fixed nuclei, focusing solely on electronic motion [5,11] or ignoring the electronic continuum, studied only the nuclear motion [12], with only few exceptions [13].

Our three-dimensional (3D) quasiclassical model entails the following steps. First, we set up the initial electronic phase space distribution. We consider parallel alignment between the molecular axis and the laser electric field (along the z axis) to directly compare with the experimental results in Ref. [8]. The field is taken to be $E(t) = E_0(t)\cos(\omega t)$ at 800 nm, corresponding to $\omega = 0.057$ a.u. (a.u. denotes atomic units). In our simulation the pulse envelope $E_0(t)$ is defined as $E_0(t) = E_0$ for $0 < t < 10T$ and $E_0(t) = E_0\cos^2[\omega(t - 10T)/8]$ for $10T < t < 12T$, with T the period of the field. We start the time propagation at $\omega t_0 = \phi_0$, where the phase of the laser field ϕ_0 is chosen randomly—see Refs. [14–16]. If the instantaneous field strength at phase ϕ_0 is smaller than the threshold field strength for over-the-barrier ionization, we assume that one electron (electron 1) tunnel ionizes, i.e., tunnels through the field-lowered Coulomb potential to the continuum, whereas the initially bound electron (electron 2) is described by a one-electron microcanonical distribution. If the instantaneous field strength at phase ϕ_0 allows for over-the-barrier ionization, we use a double-electron microcanonical distribution (see Ref. [15]). For both intensity regimes we use the tunneling rate provided by the semiclassical formula in Ref. [17] with field strength equal to that at instant t_0. We use 0.57 a.u. (1.28 a.u.) as the first (second) ionization potentials.

Second, we take the initial vibrational state of the nuclei to be the ground state ($E_0 \approx 0.01$ a.u) of the Morse potential $V_M(R) = D(1 - e^{-\beta(R-R_0)})^2$, with R the internuclear distance, $D = 0.174$ a.u., $\beta = 1.029$ a.u., and $R_0 = 1.4$ a.u. (equilibrium distance) [18]. We choose the Wigner distribution of the above state [18] to describe the initial state of the nuclei. The intensities considered in this Rapid Communication are high enough to justify restricting the initial distance of the nuclei to R_0 [19].

Third, we transform to a system of "regularized" coordinates [20,21]. This transformation explicitly eliminates the Coulomb singularity [15]. We propagate the full four-body Hamiltonian in time using the classical trajectory Monte Carlo method [22]. During time propagation, we allow the initially bound electron to tunnel at the classical turning points along the field axis using the WKB approximation—for details see

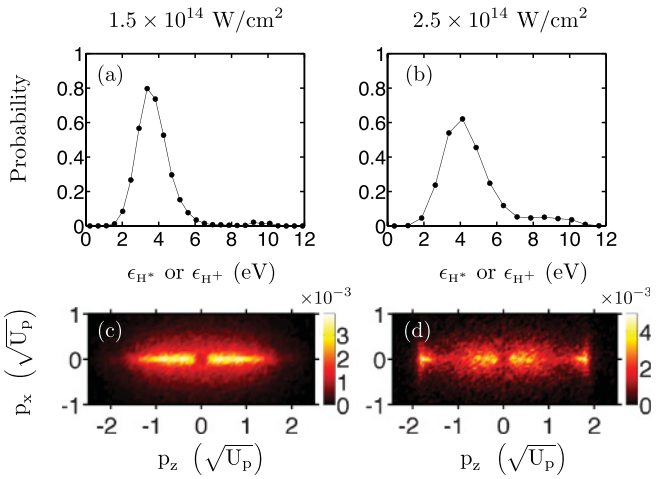

FIG. 1. (Color online) Top row: Final energy distribution of the H^+ or H^* fragments, in the H^* formation channel. Bottom row: 2D electron momentum distribution of the escaping electron, expressed in units of $\sqrt{U_p}$ [$U_p = E_0^2/(4\omega^2)$].

Ref. [23]. We finally select those trajectories leading to a breakup of H_2 with H^+, H^* (where $*$ denotes an electron in a $n > 1$ quantum state), and a free electron as fragments. To identify the electrons captured in a Rydberg n quantum state of H^*, we first find $n_c = 1/\sqrt{2|\epsilon|}$, where ϵ is the total energy of the electron. Next, we assign a quantum number so that it satisfies $[(n-1)(n-1/2)n]^{1/3} \leqslant n_c \leqslant [n(n+1/2)(n+1)]^{1/3}$, derived in Ref. [24]. We find that the distribution of principal quantum numbers n in H^* peaks at approximately $n = 8$ (not shown) resembling results for atoms [10].

To study the intensity dependence of H^* formation, we consider an intensity of 1.5×10^{14} W/cm^2 in the tunneling regime and an intensity of 2.5×10^{14} W/cm^2 in the over-the-barrier regime; however, for the latter intensity, most of the trajectories are initiated with the tunneling model. We compute the final energy distribution of the H^+ or H^* fragments for both intensities [see Figs. 1(a) and 1(b)] with at least 20 000 H^* events. The maximum of the final energy distribution at approximately 3.5 eV is in very good agreement with the experimental results in Ref. [8] (the experimental peak at approximately 0.5 eV due to bond softening is not addressed in this Rapid Communication). For the higher intensity the final energy distribution is shifted toward higher energies [compare Fig. 1(a) with Fig. 1(b)] since with increasing intensity the nuclei Coulomb explode at smaller internuclear distances. The two-dimensional (2D) momentum distributions of the escaping electron along (p_z) and perpendicular (p_x) to the laser field significantly change as we transition from the lower intensity [Fig. 1(c)] to the higher one [Fig. 1(d)]. To understand this intensity dependence we are going to identify the possible routes of forming H^* and their individual contribution to the 2D momentum distribution.

The pathways to H^* formation can be categorized as to which one of the two ionization steps, i.e., the earlier tunnel ionization of electron 1 or the later tunnel ionization of electron 2, is "frustrated." In Fig. 2(a) we show pathway A where electron 1 tunnel ionizes, subsequently escaping very quickly. Electron 2, later, tunnel ionizes and quivers in the laser field;

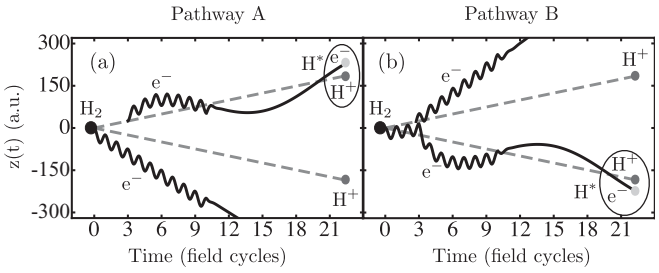

FIG. 2. Schematic illustration of the two routes leading to formation of H^*: (a) Pathway A, (b) pathway B. Shown is the time-dependent position along the laser field for electrons (black lines) and ions (gray dashed lines).

however, when the field is turned off, electron 2 does not have enough drift energy to escape and occupies a Rydberg state of the H atom instead. Hence, in pathway A the later ionization step is "frustrated." In Fig. 2(b) we show pathway B where electron 1 tunnel ionizes very quickly, quivering in the field, while electron 2 tunnel ionizes and escapes after a few periods of the laser field. When the laser field is turned off, electron 1 does not have enough energy to escape and remains in a Rydberg state of the H atom instead, i.e., the earlier ionization step is "frustrated."

We now show that these two pathways have distinct traces in the observable momentum space of the escaping electron. Figure 3 shows the two-dimensional momentum distributions of the escaping electron, for the two intensities and separate for each H^* pathway. We fix the direction of tunnel ionization of electron 1 to the left, i.e., $p_{1,z} < 0$. Comparing Fig. 3(a) with Fig. 3(b) for 1.5×10^{14} W/cm^2 and Fig. 3(e) with Fig. 3(f) for 2.5×10^{14} W/cm^2, we find that p_x,p_z of the escaping electron have a small spread in pathway A and a large spread (especially p_z) in pathway B.

Do the 2D momentum distributions change with intensity for each pathway? Comparing Fig. 3(b) with Fig. 3(f), we find that in pathway B a change in intensity from 1.5×10^{14} to 2.5×10^{14} W/cm^2 does not yield a significant change in the momentum distribution of the ionized electron 2. However, in pathway A an intensity dependence is observed in the momentum distribution of the ionized electron 1. For the lower intensity [Fig. 3(a)] electron 1 escapes mostly opposite ($p_z > 0$) to its tunnel ionization direction, while for the higher intensity [Fig. 3(e)] no directional correlation to the tunnel ionization direction can be established. This change in momentum comes along with H^* forming at a different phase of the field, ϕ_0: At approximately 0° for lower intensity [Fig. 3(c)] and at approximately ±30° for the higher intensity [Fig. 3(g)]. In Fig. 3(e), $p_z < 0$ corresponds to $\phi_0 \approx -30°$ and $p_z > 0$ to $\phi_0 \approx 30°$. The reason H^* forms when ϕ_0 shifts from small values (extrema of the field) to larger values with increasing intensity is the onset of saturated ionization of the neutral molecule [15]. According to the three-step model [25], neglecting two-electron effects, we know that electron 1 returns to the core if $\phi_0 > 0$ and does not if $\phi_0 < 0$. Similarly, our results in Fig. 3(e) show that for the higher intensity the escape direction depends on the sign of ϕ_0. This suggests that, if present, electronic correlation is weak. Hence, the differences between the lower [Fig. 1(c)] and the higher

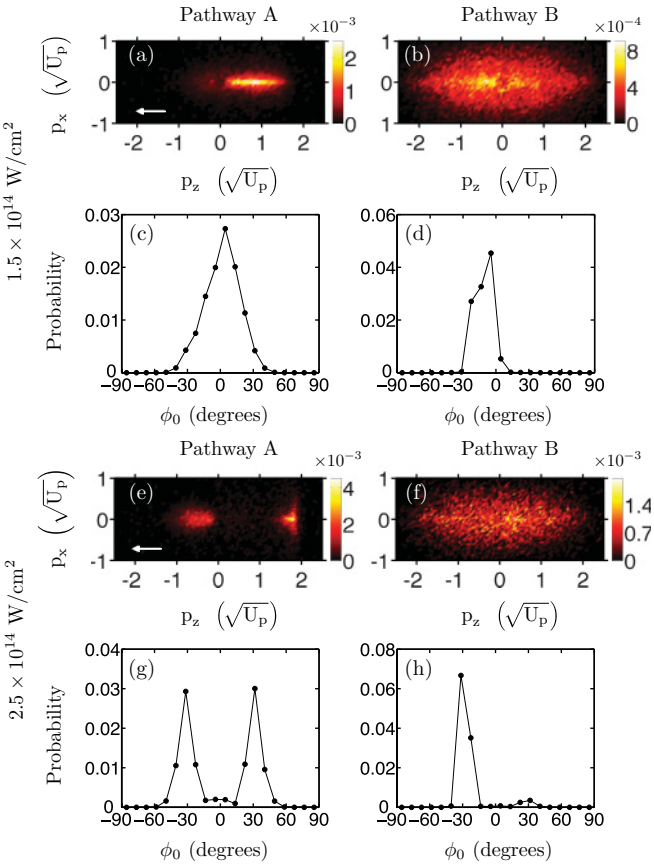

FIG. 3. (Color online) 2D electron momentum distribution of the escaping electron expressed in $\sqrt{U_p}$ for pathways A and B. The white arrow in (a) and (e) denotes the direction of tunnel ionization of electron 1. We also plot the distribution of the laser field phase ϕ_0 at the time when electron 1 tunnel ionizes in the initial state for both pathways. Accounting for tunnel ionization of electron 1 to the right as well and adding (a) and (b) yields Fig. 1(c) while adding (e) and (f) yields Fig. 1(d).

intensity [Fig. 1(d)] in the total 2D momentum distribution of the escaping electron are due to pathway A.

We now ask how electron 2 gains energy to either transition from the ground state of the H_2 molecule to a high Rydberg state of the H atom (pathway A) or escape (pathway B). Investigating the role of the laser field, we find that electron 2 gains energy through a strong interaction with the laser field that resembles enhanced ionization in H_2^+. This is corroborated by (i) the final energy distribution being similar for H^* formation (Fig. 1) and enhanced ionization [13] and (ii) by our finding that electron 2 preferentially tunnel ionizes when the nuclei are ~5 a.u. apart. This is roughly the distance of the nuclei when enhanced ionization [7] takes place. Thus, in pathway A electron 1 interacts with the laser field tunnel ionizing and escaping very quickly; the energy gain of electron 2 resembles "frustrated" enhanced ionization ("frustrated" since electron 2 occupies a Rydberg state instead of escaping). In pathway B, electron 1 interacts with the laser field tunnel ionizing and eventually occupying a Rydberg state while the energy gain of electron 2 resembles enhanced ionization.

The question that naturally arises next is to what extent electronic correlation through recollision contributes to H^* formation. Does electron 2 gain energy from electron 1 through a recollision process as in NSDI? As we have already observed discussing Fig. 3(e), electronic correlation in forming H^*, if present, is weak. Of the two pathways that prevail in NSDI, the direct and the delayed [26], electronic correlation is weak in the final electron momentum space for the delayed pathway. In this pathway [also referred to as recollision-induced excitation with subsequent field ionization (RESI) [27]] the recolliding electron returns to the core close to a zero of the field, transfers energy to the second electron, and one electron escapes with a delay of more than a quarter laser cycle after recollision. We thus explore whether electronic correlation in H^* formation resembles that in the delayed double-ionization pathway. We find that the 2D electron momentum distribution in the delayed pathway of NSDI resembles those of the H^* channel; electron 1 resembles the 2D momentum in Fig. 3(a) and electron 2 that in Fig. 3(b) for 1.5×10^{14} W/cm^2.

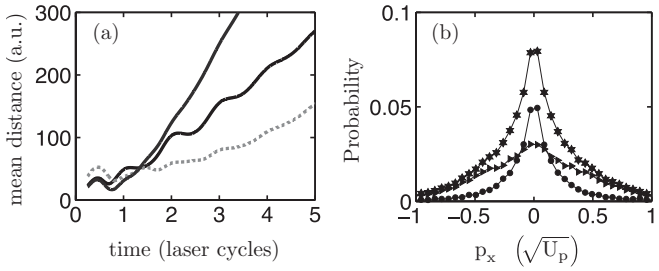

FIG. 4. (a) The mean interelectronic distance at 1.5×10^{14} W/cm^2 for pathway A (black line), pathway B (gray dotted line), and delayed pathway of NSDI (gray line). (b) The momentum distribution p_x at 1.5×10^{14} W/cm^2; total (∗), pathway A (●), and pathway B (►).

We next compute the mean interelectronic distance as a function of time—see Fig. 4(a). We find that in the delayed pathway of NSDI during recollision, at time 3/4 T, the two electrons come closer to each other as compared to pathways A and B; however, a soft recollision is present in pathway A and pathway B. On the other hand, the two electrons stay closer to each other for longer times in pathway B as compared to pathway A and to the delayed pathway in NSDI. This comparison clearly suggests that electronic correlation is present in H^* formation but mostly in pathway B. Indeed, an electron-electron interaction is more likely to occur in pathway B since electron 2 escapes while electron 1 oscillates in the vicinity of the molecular ion. Finally, we find that the probability (out of all trajectories) of pathway B reduces from 7% for the lower intensity to 3.6% for the higher one, while that of pathway A remains roughly the same, changing from 5% to 4%. This reduction of the probability for pathway B is consistent with a decrease with increasing intensity of electronic correlation in the form of recollisions. This further suggests that weak electronic correlation in the form of "frustrated" delayed NSDI contributes to forming H^* primarily in pathway B.

Finally, let us now explain the smaller spread of the momentum p_z of the ionizing electron in pathway A [Figs. 3(a) and 3(e)], rather than pathway B [Figs. 3(b) and 3(f)]. In pathway A, since mostly one-electron effects prevail, the final momentum p_z of electron 1 is primarily determined by the

value of the vector potential at the time (ϕ_0) electron 1 tunnel ionizes, resulting in a small spread in p_z due to Coulomb focusing [28]. On the other hand, in pathway B the strong interaction of electron 2 with the Coulomb potential mostly accounts for the large spread in p_z and p_x [28]. Using this difference in spread in the final momentum p_x of the escaping electron in H^* formation, one can approximately separate experimentally pathway A from B. As we show in Fig. 4(b), for the smaller intensity the electron with final momentum p_x larger than $\pm\, 0.5\sqrt{U_p}$ corresponds to primarily the escaping electron in pathway B.

Concluding, we have found that two pathways contribute to H^* formation. In pathway A, where electron 1 escapes very quickly, one electron effects prevail. Electron 2 gains energy, eventually occupying a Rydberg state, mainly through a strong interaction with the laser field resembling "frustrated" enhanced ionization in H_2^+ as conjectured in Ref. [8]. In pathway B, electron 2 escapes later by gaining energy through a strong interaction with the laser field plus a weak interaction with the other electron; the former interaction resembles enhanced ionization in H_2^+ while the latter "frustrated" delayed NSDI in H_2. This is the case for lower intensities. For higher intensities in the over-the-barrier regime, electronic correlation diminishes in both pathways while a gain of energy through strong interaction with the laser field prevails. We emphasize that the 3D quasiclassical method we developed for describing breakup channels during Coulomb explosion for strongly driven H_2 is general. It will be used in the future to explore the breakup of strongly driven multicenter molecules.

A.E. acknowledges support from EPSRC Grant No. H0031771, NSF Grant No. 0855403, and Teragrid computational resources Grant No. PHY110017. We are grateful to P. Corkum, A. Saenz, and S. Patchkovskii for discussions.

[1] A. Giusti-Suzor, X. He, O. Atabek, and F. H. Mies, Phys. Rev. Lett. **64**, 515 (1990).
[2] A. Zavriyev, P. H. Bucksbaum, H. G. Muller, and D. W. Schumacher, Phys. Rev. A **42**, 5500 (1990).
[3] A. Staudte *et al.*, Phys. Rev. A **65**, 020703(R) (2002).
[4] H. Sakai *et al.*, Phys. Rev. A **67**, 063404 (2003).
[5] A. S. Alnaser *et al.*, Phys. Rev. Lett. **91**, 163002 (2003).
[6] H. Niikura *et al.*, Nature (London) **417**, 917 (2002).
[7] T. Zuo and A. D. Bandrauk, Phys. Rev. A **52**, R2511 (1995); T. Seideman, M. Y. Ivanov, and P. B. Corkum, Phys. Rev. Lett.**75**, 2819 (1995); D. M. Villeneuve, M. Y. Ivanov, and P. B. Corkum, Phys. Rev. A **54**, 736 (1996); E. Dehghanian, A. D. Bandrauk, and G. L. Kamta, *ibid.* **81**, 061403 (2010).
[8] B. Manschwetus *et al.*, Phys. Rev. Lett. **102**, 113002 (2009).
[9] T. Nubbemeyer, U. Eichmann, and W. Sandner, J. Phys. B **42**, 134010 (2009); B. Manschwetus *et al.*, Phys. Rev. A **82**, 013413 (2010); B. Ulrich *et al.*, *ibid.* **82**, 013412 (2010).
[10] T. Nubbemeyer, K. Gorling, A. Saenz, U. Eichmann, and W. Sandner, Phys. Rev. Lett. **101**, 233001 (2008).
[11] M. Awasthi and A. Saenz, J. Phys. B **39**, S389 (2006).
[12] J. McKenna *et al.*, Phys. Rev. Lett. **100**, 133001 (2008).
[13] H. A. Leth, L. B. Madsen, and K. Molmer, Phys. Rev. Lett. **103**, 183601 (2009); F. Martin *et al.*, Science **315**, 629 (2007).
[14] A. Emmanouilidou, Phys. Rev. A **78**, 023411 (2008).
[15] A. Emmanouilidou and A. Staudte, Phys. Rev. A **80**, 053415 (2009) and references therein for the initial electronic state.
[16] J. Chen, J. Liu, L. B. Fu, and W. M. Zheng, Phys. Rev. A **63**, 011404(R) (2000); T. Brabec, M. Y. Ivanov, and P. B. Corkum, *ibid.* **54**, R2551 (1996).
[17] Y. Li, J. Chen, S. P. Yang, and J. Liu, Phys. Rev. A **76**, 023401 (2007).
[18] A. Frank, A. L. Rivera, and K. B. Wolf, Phys. Rev. A **61**, 054102 (2000).
[19] A. Saenz, Phys. Rev. A **61**, 051402(R) (2000).
[20] P. Kustaanheimo and E. Stiefel, J. Reine Angew. Math. **218**, 204 (1965).
[21] D. C. Heggie, Celestial Mech. **10**, 217 (1974).
[22] R. Abrines and I. C. Percival, Proc. Phys. Soc. **89**, 515 (1966).
[23] J. S. Cohen, Phys. Rev. A **64**, 043412 (2001); for the WKB transmission probability, see Eugen Merzbacher, *Quantum Mechanics* (Wiley, New York, 1998), Chap. 7.
[24] R. L. Becker *et al.*, J. Phys. B **17**, 3923 (1984).
[25] P. B. Corkum, Phys. Rev. Lett. **71**, 1994 (1993).
[26] A. Emmanouilidou *et al.*, New J. Phys. **13**, 043001 (2011).
[27] R. Kopold, W. Becker, H. Rottke, and W. Sandner, Phys. Rev. Lett. **85**, 3781 (2000); B. Feuerstein *et al.*, *ibid.* **87**, 043003 (2001).
[28] D. Comtois *et al.*, J. Phys. B **38**, 1923 (2005).